linear array of eight mirrors was repeatedly actuated and clamped into the up position. A HeNe laser was used to determine mirror angle with respect to the substrate to an accuracy of 0.01°. Figure 5 shows results for multiple actuations of each of the eight mirrors. Results demonstrate pointing accuracy with a mirror-to-mirror standard deviation of 0.06° and individual 1-sigma mirror repeatability of 0.008°.

Reliability

Another important aspect of the MagOXC is its reliability with respect to hinge fatigue, shock, and effects of stiction. Design of an effective hinge necessitates trade-offs between hinge robustness and mechanical compliance. The hinge needs to be flexible to permit full mirror rotation with the relatively weak actuation force, yet be resistant to fatigue effects and stresses produced by shock and vibration. We will report results of cyclic mirror actuation to demonstrate fatigue and wear resistance. We will also report results from six-axis shock testing up to 500G to demonstrate compliance with Telcordia GR-1221 requirements. Stiction effects arise in microstructures when adhesion forces overtake applied actuation forces. Since the MagOXC relies on contact of the mirror with banking wall to effect passive alignment, specific design features are incorporated to prevent this contact from producing stiction in use. Cyclic testing is configured to detect missed switch cycles caused by stiction.

TuO3 2:45 pm

A Low Voltage, Large Scan Angle MEMS Micromirror Array with Hidden Vertical Comb-Drive Actuators for WDM Routers

Dooyoung Hah, Sophia Huang, Hung Nguyen, Hsin Chang, and Ming C. Wu, *Department of Electrical Engineering, University of California, Los Angeles, Box 951594, Los Angeles, CA 90095-1594, Email: hady@icsl.ucla.edu*

Hiroshi Toshiyoshi, *Institute of Industrial Science, University of Tokyo, 4-6-1 Komaba, Meguro-ku, Tokyo 153-8505, Japan*

1. Introduction

The evolution of photonic communication networks towards optical layer networking has created a great demand for many new functional optical network elements. Microelectromechanical-systems (MEMS) is a key enabling technology for many of these new devices. Dynamic optical add-drop multiplexers (OADM),[1] 2-D[2] and 3-D optical crossconnect[3] have been demonstrated. In this paper, we report a new surface-micromachined 1-D micromirror array that has applications in WDM routers and wavelength-selective crossconnect (WSXC). Using novel vertical comb-drive actuators hidden under the micromirrors, large continuous scan range (24°), low operating voltage (9 V), and high linear fill factor (91%) have been achieved.

The schematic diagram of the proposed WDM router is shown in Fig. 1(a). M collimated beams are dispersed by a grating, and then focused onto a linear array of micromirrors. Scanning of the micromirrors allows individual wavelength to be switched between any two fibers independently. The WDM router can be configured as a wavelength-selective 1 × N switch, or as a multi-port OADM. It can also be used as a basic building block for WSXC.

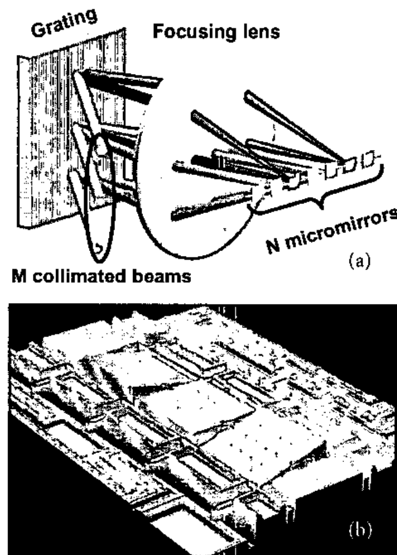

TuO3 Fig. 1. (a) Schematic diagram of the WDM router and (b) an optical interferometric image (by WYKO) of the fabricated micromirror array. Two of the micromirrors have been tilted by actuators.

2. MEMS Micromirror Arrays

Fig. 1(b) shows the optical interferometric image of the fabricated 1 × 10 micromirror array. Two of the mirrors have been tilted by actuators. The micromirror array has very high fill factor along the array direction (91%), which is important to achieve flat-top spectral response.[4] This is made possible by placing both actuators and torsion springs underneath the mirror. The schematic structure of our micromirror is shown in Fig. 2(a). Vertical comb-drive actuators are used to reduce the operating voltage and extend the linear scan range. Unlike conventional parallel-plate type electrostatic actuators, the comb-drive actuators do not suffer from the pull-in effect and can fully utilize the entire scan range. The vertical comb-drives also have higher electrostatic torque, which enables low voltage operation. Bulk-micromachined vertical comb-drives have been reported.[5,6] Both the comb-drive actuators and the torsion springs are placed under the mirror to achieve high fill factor.

The micromirror array was fabricated by SUMMiT-V (Sandia Ultra-planar Multilevel MEMS Technology-V) process. The SUMMiT-V process has four structural polysilicon layers and four sacrificial oxide layers, which are ideal to implement our micromirrors. In addition, the top two polysilicon layers (poly3 and poly4) are deposited on chemical-mechanical-planarized (CMP) oxide layers so that underlying topography will not replicate on the top layers. This feature is critical for fabricating vertical comb-drive actuators underneath the flat micromirrors. The spring and the mirror are made of poly1 and poly4, respectively. The movable fingers are made of poly3 and the fixed fingers are made of laminated poly1 and poly2. After fabrication, the mirrors are released in HF for 45 minutes at room temperature. Cr/Au is deposited by maskless e-beam evaporation to increase the mirror reflectivity. Electrical isolation between electrodes was achieved by incorporating overhang structures.

Fig. 2(b) shows the SEM image of the fabricated micromirror. Half of the mirror was intentionally removed to show the underlying comb-drive actuators. Despite the complicated underlying structure, the mirror surface remains flat. The mirror has an area of $137 \times 120\ \mu m^2$ and a pitch of 150 μm, yielding a fill-factor of 91%. The radius of curvature of the mirror was measured to be 35 mm. Each comb-drive actuator has 36 fingers. The finger width and the spacing are both 1 μm. The spring dimension is 1 (thickness) × 1 (width) × 55 (length) μm^3.

The DC scanning characteristic of the micromirror was measured using WYKO, a non-contact surface profiler with laser interferometry.

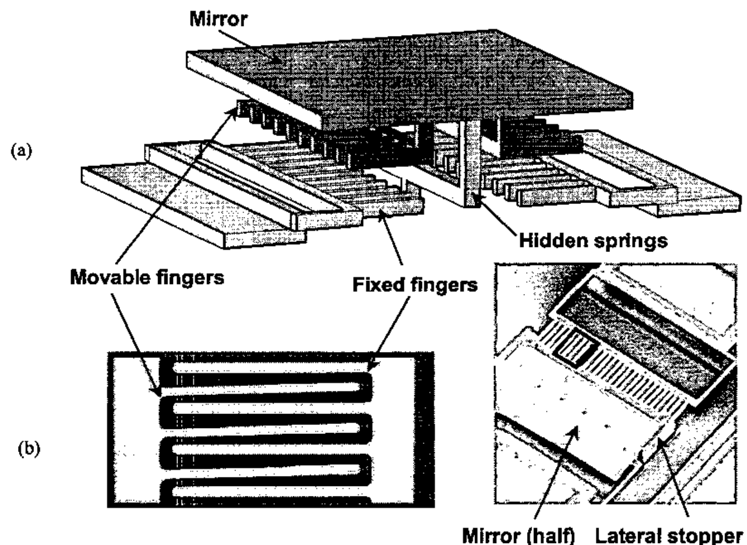

TuO3 Fig. 2. (a) Schematic diagram and (b) SEM images of the micromirror. Half of the micromirror is intentionally removed to show the underlying vertical comb structures. The inset is the magnified view of the vertical comb fingers.

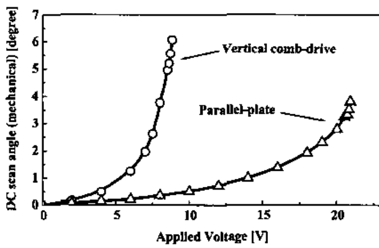

TuO3 **Fig. 3.** Measured DC scanning characteristics of the micromirror with vertical comb-drive actuator (circle) and with parallel-plate actuator (triangle).

Fig. 3 shows the measured result. The mirror is tilted by 6° (mechanical angle) with 9 V bias. The total optical scan angle is 24°. Good uniformity (±5%) across the array is obtained. For comparison, a parallel-plate-actuated micromirror with the same mirror size, spring dimension, and mirror height was also fabricated on the same wafer. The scanning characteristic is shown in Fig. 3 as well. It has smaller scan angle (3.8°) and much higher operating voltage (21 V).

3. WDM Routers

The WDM router in Fig. 1(a) is currently under test. The current system employs a two-inch lens with a focal length of 150 mm and a grating of 600 lines/mm. This initial system can accommodate 6 spatial channels and 10 wavelength channels. The calculated beam waist on micromirror (ω_{mirror}) is 36 μm with the beam waist of collimator (ω_{col}) of 2 mm. The performance of the system was analyzed by using Gaussian beams and ZEMAX. The optical insertion loss of the system is estimated to be less than 1.5 dB, with less than 0.3 dB variations across the spatial channels and less than 0.1 dB variations across all wavelength channels. Larger number of spatial and wavelength channels can be achieved by employing 2-D arrays of spatial channels and 2-axis scanning micromirror arrays.

4. Conclusion

A MEMS micromirror array with hidden vertical comb-drive actuator and springs has been successfully demonstrated. The devices were fabricated using SUMMiT-V process. The fabricated micromirror showed large optical scan angle (24°) and low actuation voltage (9 V). The fill-factor of the micromirror array was as high as 91%. Applications of the micromirror array for WDM routers are also discussed.

References

1. J.E. Ford, V.A. Aksyuk, David J. Bishop, and J.A. Walker, "Wavelength add-drop switching using tilting micromirrors," J. Light. Technol., 17, 904–911 (1999).
2. A. Husain, "MEMS-based photonic switching in communications networks," in OFC 2001, Paper WX1.
3. R. Ryf, et al., "1296-port MEMS Transparent Optical Crossconnect with 2.07 Petabit/s Switch Capacity," in OFC 2001, Postdeadline Paper PD28.
4. J.S. Patel and Y. Silberberg "Liquid crystal and grating-based multiple-wavelength crossconnect switch," IEEE Photon. Technol. Lett., 7, 514–516 (1995).
5. S. Miller, K. Turner, and N. Macdonald, "Microelectromechanical scanning probe instruments for array architectures," Rev. Sci. Instrum., 68, 4155–4162 (1997).
6. J.-L.A. Yeh, H. Jiang, and N.C. Tien, "Integrated polysilicon and DRIE bulk silicon micromachining for an electrostatic torsional actuator," J. Microelectromech. Syst., 8, 456–465 (1999).

TuO4 **3:00 pm**

Digital MEMS switch for planar photonic crossconnects

Li Fan, S. Gloeckner, P.D. Dobblelaere, S. Patra, D. Reiley, C. King, T. Yeh, J. Gritters, S. Gutierrez, Y. Loke, M. Harburn, R. Chen, E. Kruglick, M. Wu and A. Husain, *OMM, Inc., 9410 Carroll Park Drive, San Diego, CA 92121, USA, lifan@omminc.com*

1. Introduction: Planar optical crossconnects

Optical switches are data rate and protocol independent, which makes them attractive for optical networks.[1–3] Free-space optical switches offer low loss, PDL, and cross-talk. MEMS-based approaches to miniaturize opto-mechanical switches have been proposed. They offer scalability combined with excellent optical performance. Arranging mirrors on a silicon substrate various switching functions can be performed. A functional diagram of a two-dimensional (2-D) 8 × 8 switch are shown in Figure 1. If the micro-mirrors are turned on, the light signals from Plane 1 can be directed to outputs in Plane 2. When the mirrors are off, then the light from Plane 1 can pass through to outputs in Plane 4. This architecture is called 2D because it uses N^2 individual mirrors and switch cells, e.g., 256 devices for a 16 × 16 switch. The main elements of the MEMS switch cell are the mirror and the actuator. The mechanical design of the switch cell determines the optical characteristics of the component.

2. Design of a digital MEMS switch

For fiber-optical switches, the challenges are how to obtain large travel distance, high accuracy and repeatable angle as well as fast switching speed at the same time. Especially for large array such as 16 × 16, the collimator beam waist could be larger than 100 μm. The actuator design needs to be able to provide repeatable traveling distance more than several hundred microns in order to completely switch the mirrors on and off. Comb drives have been proven to be reliable actuators. However, it would be difficult to actuate long distance with small footprint by surface micro-machine process. Thermal actuators and scratch drive actuators are not considered because of long-term reliability and repeatability issues. Piezoelectric actuation requires the use of materials with high piezoelectric effect, such as zinc oxide or lead-zirconate-tintanate (PZT), which are not readily compatible with IC fabrication techniques. Magnetic actuation can generate very large forces, but the effects are difficult to shield, making it difficult to make large arrays of independent actuators. Magnetic actuators also dissipate power near the MEMS devices. Gap-closing electrostatic actuator exploit the attraction of oppositely charged mechanical elements, and is considered one of the best candidates for actuation. Its advantages include repeatability, low power consumption and ease of shielding. It also does not require special materials.

Figure 2a shows the schematic diagram of the basic switch elements. Figure 2b photograph shows the detail structures of the mirror, actuator and the landing stopper. The gap-closing actuator plate initial angle is assembled and actuated by electro-static force from the electrodes. The mirror is assembled at 90 degrees and sits on the actuator plate. Large traveling distance is achieved by extending the actuator arm. The extended arm doesn't generate much more force. However, several hundred microns displacement can be achieved with this configuration. The switching is achieved by moving the actuator up and down. The mirror is maintained to be 90 degrees during the entire switching cycle. The mirror traveling direction is perpendicular to the optical path. This design has advantage over the pop-up mirror configuration, which rotate the mirror from

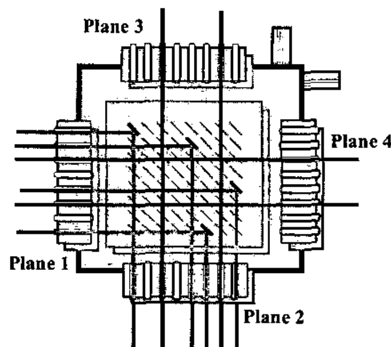

TuO4 **Fig. 1.** Switching architecture.

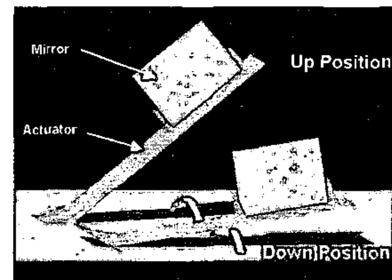

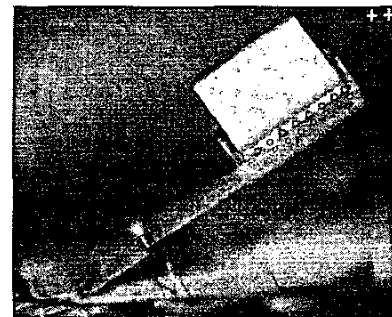

TuO4 **Fig. 2.** a). Schematic diagram of 2D MEMS switch. b). Photograph of single digital switch.